PNAS RESEARCH ARTICLE | MICROBIOLOGY CHEMISTRY

Discovery of unusual dimeric piperazyl cyclopeptides encoded by a *Lentzea flaviverrucosa* DSM 44664 biosynthetic supercluster

Chunshun Li[a,b,1,2], Yifei Hu[c,1,3], Xiaohua Wu[a], Spencer D. Stumpf[c,4], Yunci Qi[c], John M. D'Alessandro[c,5], Keshav K. Nepal[c], Ariel M. Sarotti[d], Shugeng Cao[a,b,6], and Joshua A. V. Blodgett[c,6]

Edited by Jens Nielsen, BioInnovation Institute, DK2200 Copenhagen, Denmark; received October 5, 2021; accepted March 7, 2022

Rare actinomycetes represent an underexploited source of new bioactive compounds. Here, we report the use of a targeted metabologenomic approach to identify piperazyl compounds in the rare actinomycete *Lentzea flaviverrucosa* DSM 44664. These efforts to identify molecules that incorporate piperazate building blocks resulted in the discovery and structural elucidation of two dimeric biaryl-cyclohexapeptides, petrichorins A and B. Petrichorin B is a symmetric homodimer similar to the known compound chloptosin, but petrichorin A is unique among known piperazyl cyclopeptides because it is an asymmetric heterodimer. Due to the structural complexity of petrichorin A, solving its structure required a combination of several standard chemical methods plus in silico modeling, strain mutagenesis, and solving the structure of its biosynthetic intermediate petrichorin C for confident assignment. Furthermore, we found that the piperazyl cyclopeptides comprising each half of the petrichorin A heterodimer are made via two distinct nonribosomal peptide synthetase (NRPS) assembly lines, and the responsible NRPS enzymes are encoded within a contiguous biosynthetic supercluster on the *L. flaviverrucosa* chromosome. Requiring promiscuous cytochrome p450 crosslinking events for asymmetric and symmetric biaryl production, petrichorins A and B exhibited potent in vitro activity against A2780 human ovarian cancer, HT1080 fibrosarcoma, PC3 human prostate cancer, and Jurkat human T lymphocyte cell lines with IC_{50} values at low nM levels. Cyclic piperazyl peptides and their crosslinked derivatives are interesting drug leads, and our findings highlight the potential for heterodimeric bicyclic peptides such as petrichorin A for inclusion in future pharmaceutical design and discovery programs.

rare actinomycete | *Lentzea* | cytochrome P450 | cyclopeptide | biosynthesis

Nature represents one of humankind's most important and enduring sources of therapeutics. The ability of living things to produce drug-like compounds is unevenly distributed in biology, where certain types of organisms are particularly enriched (1). Filamentous actinomycete bacteria are particularly noteworthy for this trait, producing >50% of molecular scaffolds found in clinically utilized antibiotics plus many other needed medicines (2). Drug discovery from actinomycetes and other microbes has seen a great revitalization in recent years (3). While the roots of this revitalization are complex, a combination of emerging drug scarcity, changing attitudes toward microbial bioproduction, and renewed enthusiasm for evolved molecules as drug leads were significant drivers (4).

Demands for new antibiotics are critical, with resistant and emerging infections posing a serious but largely unchallenged global health threat (5). The idea that actinobacterial products might have future roles in mitigating that threat owes primarily to the advent of increasingly affordable DNA sequencing and the development of advanced genomics toolsets (6, 7). Once thought to be largely devoid of new drugs, these technologies revealed a deep trove of yet-undiscovered drug-like molecules hidden in actinobacterial genomes (8).

However, translating genomic knowledge into molecules for clinical development has proved to be challenging (9). Many biosynthetic gene clusters (BGCs) that encode desirable molecules are thought to be "silent" (10). Silent clusters are characterized by the lack of expected chemical products, which frustrates drug development efforts. Furthermore, the computational side of drug discovery (i.e., genome sequencing, annotation, and biosynthetic prediction) now vastly outpaces the experimental capacity to prosecute all newly discovered BGCs for molecule discovery. Because of this, discovery requires the use of increasingly complex schemes to identify which bacterial strains and biosynthetic loci will most likely produce desirable molecules once pursued (7, 11).

Significance

Actinomycetes produce many clinically useful drugs, especially antibiotics and anticancer agents. Rare actinomycetes are known to produce bioactive molecules but they remain underexplored compared to more common *Streptomyces spp*. Natural molecules having piperazate building blocks are often bioactive, and genome analyses previously indicated the rare actinomycete *Lentzea flaviverrucosa* DSM 44664 may encode for the production of such molecules. To discover these from complex fermentation mixtures, we devised and employed a targeted metabolomic approach that revealed petrichorin A, an unusual heterodimeric biaryl-cyclohexapeptide. Its structure was determined by using multidimensional nuclear magnetic resonance, theoretical calculations, and strain mutagenesis, and its biosynthesis implicated an atypical cytochrome p450 heterodimerization event. Petrichorin A demonstrated potent cytotoxicity, highlighting heterodimeric-biaryls as interesting features for future drug design.

The authors declare no competing interest.

This article is a PNAS Direct Submission.

[6]To whom correspondence may be addressed. Email: scao@hawaii.edu or jblodgett@wustl.edu.

This article contains supporting information online at http://www.pnas.org/lookup/suppl/doi:10.1073/pnas.2117941119/-/DCSupplemental.

Published April 19, 2022.

Bioinformatic efforts typically scan microbial genomes for BGCs encoding molecules having known pharmacophores, privileged scaffolds, or other desirable chemical motifs. Microbial producers are selected for genome-sequencing based on equally complex criteria, including their relatedness to traditional producers of approved drugs, isolation from unique environmental niches, their relative rarity in culture collections, and other factors (12).

Piperazate (piz) is a nonproteinogenic amino acid and proline mimic that imparts conformational constraint and other desirable properties to natural and synthetic molecules that incorporate it (13). Piz fits the classical definition of a privileged scaffold, a molecular substructure associated with compounds that can target diverse biology (14). Thus, piperazyl compounds are desirable for therapeutic discovery. In addition to being counted among several known drugs and important structural leads (e.g., cilazapril, the matlystatins, and sanglifehrins) (15), piperazyl molecules have additional research interest owing to their atypical associated enzymology (16–18) and proposed roles in microbial symbiosis and chemical ecology (19–21).

There are over 100 documented natural products with integral piz moieties, most of which are produced by actinobacterial members of the *Streptomyces* genus (22). The recent elucidation of piz biosynthesis via the unusual hemoprotein KtzT and related members of the PzbB-protein family has enabled straightforward recognition of piperazyl-molecule BGCs in microbial genomes (17, 18). Our prior work on actinobacterial piperazate metabolism revealed a *pzbB*-linked BGC in *Lentzea flaviverrucosa* DSM 44664, and the enzyme it encodes was competent for piperazate production in heterologous *Streptomyces* hosts (18). *L. flaviverrucosa* is a member of the Pseudonocardia family and is a member of the so-called "rare actinomycetes" (23). Rare actinomycetes, including *Lentzea*, *Actinoplanes*, *Nonomurea*, and *Salinispora* plus several other genera, are phylogenetically diverse and biotechnologically interesting filamentous actinobacteria (23). These organisms are recognized for their potential to produce biotechnologically important molecules, but remain significantly underexplored compared to their more commonly encountered *Streptomyces* relatives (24). Understanding and accessing the biosynthetic potential of rare actinomycetes is a priority for continued natural drug discovery, but work exploring *Lentzea* for biotechnology remains relatively sparse. Known *Lentzea* products include rebeccamycin (25), lassomycin (26), and the lentzeosides (27), and members of the genus have been used for the bioconversion of the cyclosporin A-derivative FR901459 into several new congeners (28). Published examples of *Lentzea* genetic systems to support biotechnological development are also limited, with *Lentzea.* sp. strain ATCC 31319 mutations for the study of thiolactomycin production being the lone example (29).

Motivated by our earlier findings indicating *L. flaviverrucosa* should produce a yet- undiscovered piperazyl compound (18), here we report the targeted discovery of the biosynthetically atypical piperazyl compounds petrichorins A and B (Fig. 1) from this strain. Identifying these molecules in growth extracts was enabled by combination pzbB gene disruptions, *L*-orn isotopic-labeling, and piperazyl-targeting tandem mass spectrometry (MS/MS) fragmentation analysis. After fully resolving their structures, both petrichorins were found to share several structural features with a growing family of cyclic peptides and depsipeptides (including chloptosin [30], himastatin [31], and members of the alboflavusin [32, 33] and kutzneride [34] complexes) (Fig. 1, *Top*) that incorporate both piperazyl and hydroxyhexahydropyrrolo[2,3-*b*]indole-2-carboxamide (HPIC) substructural elements. Of the two petrichorins, the minor product petrichorin B was more structurally simplistic, consisting of a bicyclic-cyclopeptide homodimer whose structure is highly similar to chloptosin. By comparison, the major product petrichorin A significantly differed from all previously known dimeric cyclohexapeptides in that it is a heterodimer comprised of one half of petrichorin B crosslinked to a different cyclohexapeptide, named petrichorin C (Fig. 1, *Bottom*). The biosynthesis of the petrichorins was pursued via additional genetic experiments in the native host, revealing that the production of the highly atypical asymmetric dimer petrichorin A requires an unusual cytochrome p450 crosslinking of two different cyclopeptides generated by distinct NRPS assembly lines. Finally, the bioactivites of petrichorins A, B, and C were tested against human HT1080 fibrosarcoma, PC3 prostate cancer, A2780 ovarian cancer, and Jurkat T lymphocyte cell lines. The petrichorin A heterodimer showed significant inhibition along with the B homodimer, and both of these were superior to the C monomer. Accordingly, we posit that heterodimeric biaryl-cyclohexapeptides and their depsipeptide analogs should be specifically considered for future therapeutic-lead synthesis.

Results and Discussion

Piperazate-Targeted Metabologenomics for Petrichorin Discovery. Piperazate biosynthesis requires the formation of an unusual *N–N* bond, which is formed by heme b-dependent enzymes related to KtzT. We previously identified and heterologously expressed a *ktzT* ortholog from *L. flaviverrucosa* (*ltzT*) that produces piperazate in recombinant *Streptomyces lividans* and *Streptomyces flaveolus* (18). This suggested that *L. flaviverrucosa* likely has the native capacity to produce piperazyl compounds but none had been discovered in this strain or in any other *Lentzea spp*. Examining the *ltzT* gene neighborhood revealed a potential biosynthetic gene cluster (BGC, ~67 kb, *ltzA-ltzV*) encoding multiple predicted tryptophan halogenases, five NRPS enzymes having 11 total adenylation domains, a single transcriptional regulator, transporters, and several oxidative tailoring genes (Fig. 2*A*, *SI Appendix*, Table S1).

To discover piperazyl molecules in *L. flaviverrucosa*, we used a multipronged approach based on the genetics of piz monomer production and piperazate-targeted metabolomics (Fig. 2 *B–D*). Piz biosynthesis from L-ornithine (*L*-orn) requires an *N*-hydroxylase and an *N*-hydroxy-*L*-orn cyclase, and homologs of both were found in the *ltz* locus (Fig. 2*A*, *ltzF* and *ltzT*, respectively). Thus, we tested *L. flaviverrucosa* for a metabolic response to exogenous *L*-piz and d^7-*L*-orn to identify potential piperazyl compounds. After feeding the strain with these amino acids, organic extracts of spent growth media were analyzed via liquid chromatography/mass spectrometry (LC/MS), revealing a single strong peak that responded positively to both compounds (Fig. 2 *B* and *C*). Specifically, exogenous L-Piz approximately doubled the peak area of one *L. flaviverrucosa* metabolite (0.5–1 mM supplementation), and the same piz-responsive signal also incorporated deuterated-*L*-orn, consistent with a piperazyl metabolite.

We then utilized an MS/MS fragmentation scheme for more sensitive detection of piperazyl compound signals within complex microbial extracts. This method was established using matlystatin production in *Amycolatopsis atramentaria* (35, 36), where MS/MS was used to identify daughter ions containing the piperazyl-feature of matlystatin B via d^7-*L*-Orn incorporation (*SI Appendix*, Fig. S1). By comparing labeled vs. unlabeled extracts, we identified a piperazate-derived *m/z* 85.1 fragment, which we surmised could be used for the sensitive detection of other piperazyl compounds. After applying this method to

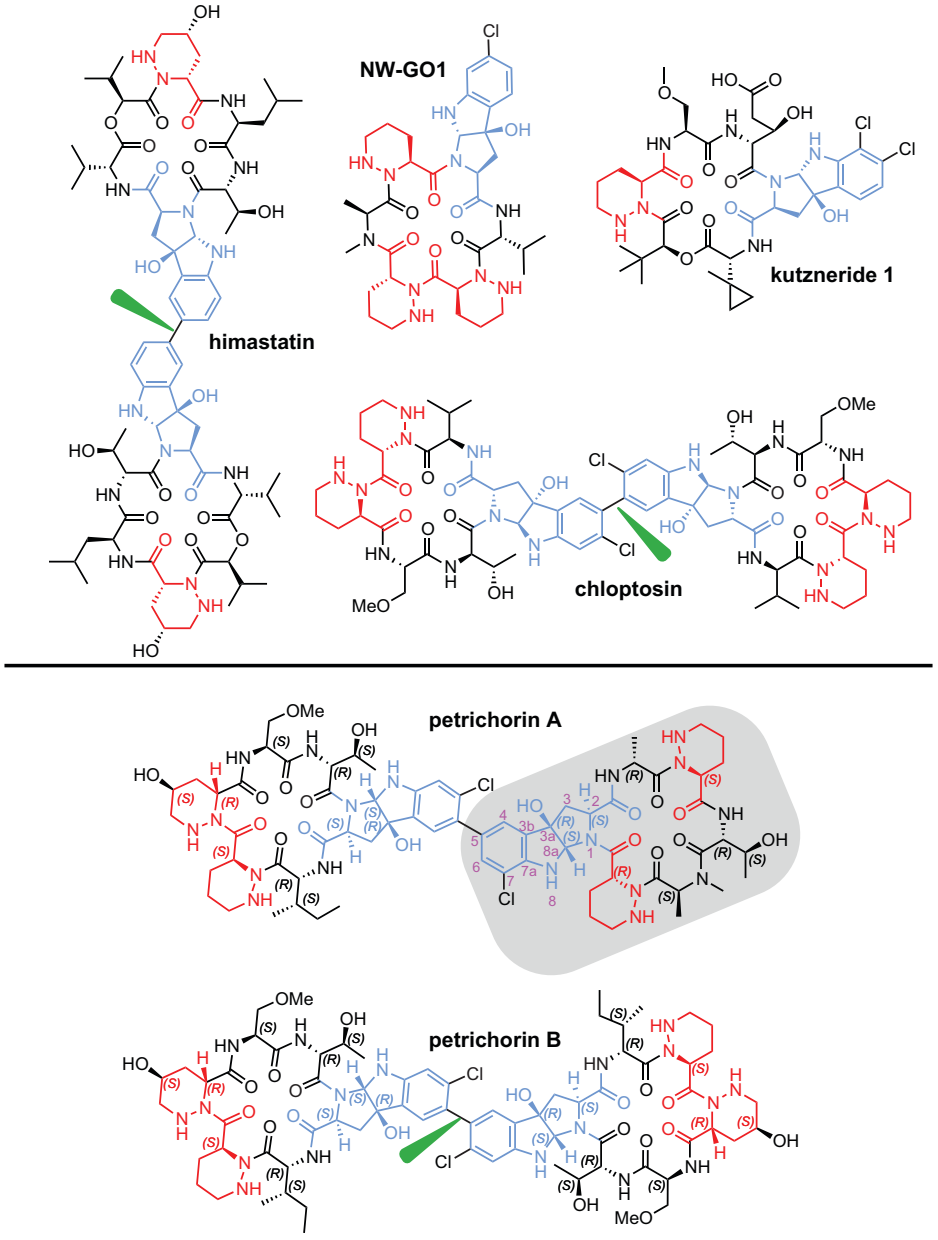

Fig. 1. Actinobacterial piperazyl cyclic(depsi)peptides. (*Top*) Several naturally occurring cyclic peptides having HPIC (blue) and piz (red) substituents are known from the literature. Many examples are monomeric, including kutzneride 1 and the alboflavusin congener NW-GO1. Natural homodimers in the class are also known (e.g., himastatin and chloptosin). The homodimers are comprised of identical monomers symmetrically coupled via (chloro)biaryl linkages (green darts). (*Bottom*) Structures of petrichorins A and B discovered herein. Petrichorin A is heterodimeric; each cyclopeptide half of the chlorobiaryl is structurally distinct. The left cyclopeptide of petrichorin A is identical to that making up the homodimer petrichorin B. The right cyclopeptide constituent of petrichorin A (gray background) was later identified as a monomer, petrichorin C, that accumulates in certain deletion mutants; see text.

L. flaviverrucosa, we rediscovered the piz-responsive signal from Fig. 2*B*, plus an additional minor product missed by our initial efforts (Fig. 2*D*).

To confirm these molecules are indeed piz-dependent and encoded by the *ltz* locus, we established a genetic system in *L. flaviverrucosa* to create unmarked gene deletions. This was achieved using a standard *rpsL*-counterselection approach (see *Materials and Methods*), and all mutants described herein were created in the same *rpsL* background (S12 K88M, JV691). After deleting piz-essential *ltzT*, the resulting mutant was deficient for both peaks identified in Fig. 2*D*. Both signals were rescued by ectopically expressing *ltzT* under the control of the strong constitutive promoter P*ermE**. Other *ltzT* orthologs cloned from piperazyl BGCs in *Kutzneria* sp strain 744 (*ktzT*, kutznerides) and *Streptomyces himastatinicus (hmtC*, himastatin) similarly restored function (Fig. 2*D*). These data clearly linked the production of the Fig. 2 piperazyl signals to the *ltz* locus.

Structure of the Petrichorins. Both molecules detected in Fig. 2*D* were purified to homogeneity for structural elucidation (see *Materials and Methods* and *SI Appendix*). Both were isolated as white powders, and HR-ESI-MS revealed each had distinct masses and mass formulae (the major product, petrichorin A, $C_{67}H_{92}Cl_2N_{18}O_{18}$ *m/z* 1507.6288, calculated for $[M + H]^+$ 1507.6287; the minor product petrichorin B, $C_{70}H_{98}Cl_2N_{18}O_{20}$ quasi-molecular ion peak at *m/z* 1603.6484 $[M + Na]^+$, calculated 1603.6474).

NMR characterization of petrichorin A was challenging due to extensive signal overlap. Pursuing the final structure of this molecule thus required a combination of standard 1D and 2D

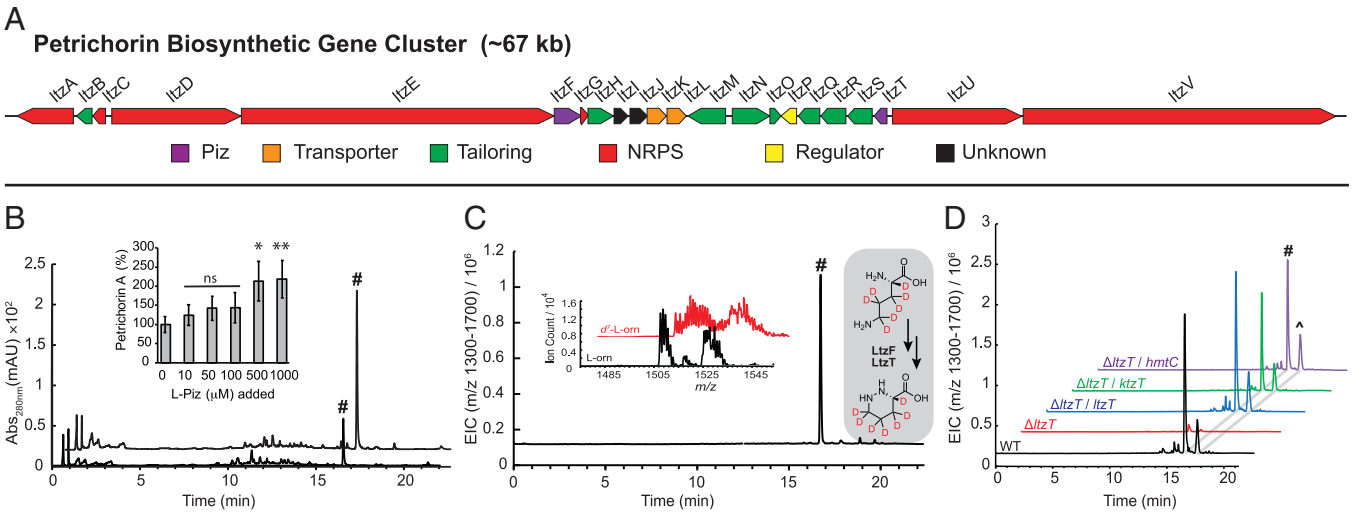

Fig. 2. Petrichorin discovery via targeted metabologenomics. (*A*) Open reading frame map of the *L. flaviverrucosa ltz* locus, a biosynthetic supercluster that encodes for the petrichorins. Piperazate biosynthetic genes *ltzF* and *ltzT* are centrally positioned within the cluster (purple), which is predominantly made up of genes encoding for NRPS enzymology, tailoring, and regulatory functions indicated in the color key. (*B*) UV-HPLC analysis of *L. flaviverrucosa* organic extracts revealed a Piz-responsive peak (#), which (*C*) also showed evidence of d^7-*L*-orn incorporation by mass-envelope broadening following MS analysis. Consistent with piperazyl compound biosynthesis (see *C, Inset* labeling scheme), (*D*) piperazyl-targeted HPLC-MS/MS revealed the same major peak found in *B* and *C* (#, petrichorin A) plus a minor, later eluting peak (^, petrichorin B). Both molecules are lost by deleting *ltzT* and both were rescued by ectopic expression of *ltzT* or its orthologs *ktzT* and *hmtC*. Error bars in (*B*) indicate SD.

NMR and other chemical methods (*SI Appendix* and Table S2), plus in silico modeling and strain mutagenesis for confident structural assignment (latter discussed below). In brief, comprehensive 2D-NMR analysis (COSY, TOCSY, HSQC, and HMBC) (*SI Appendix*, Figs. S2–S8) suggested the presence of one alanine (ala), one *N*-methyl-alanine (*N*Me-ala), one isoleucine (ile), one *O*-methyl-serine (*O*Me-ser), two threonines (thr-1 and thr-2), four piperazic acids (one being hydroxylated at γ-position), plus two chlorinated tryptophan (trp) derivatives (later identified as HPIC). Amino acid hydrolysis followed by Marfey's analysis (37) indicated the absolute configuration of the component amino acids (*SI Appendix*, Figs. S9–S16), and HMBC and NOESY were used to determine amino acid sequences for both the asymmetric left and right rings of petrichorin A (*SI Appendix*, Fig. S28). Additionally, Mosher reactions coupled with 2D NMR (38) were used to determine the absolute configuration of secondary alcohols (*SI Appendix*, Figs. S17–S27). Finally, the absolute configurations of the asymmetrically chlorinated and cross-linked HPIC residues of heterodimeric petrichorin A required quantum calculations of NMR shifts, an established strategy to resolve difficult natural product structures (39). To do this with minimized computational cost, we theoretically modeled four simplified bicyclic HPIC derivatives (*SI Appendix*, Figs. S29, *isomers* 1*a–d*, and S30) and correlated calculated shifts with collected experimental values for the analogous region of petrichorin A. Following systematic conformational sampling at the MMFF level, followed by fast NMR calculations at B3LYP/6–31G** the *J*-DP4 calculations suggested (*SI Appendix*, Fig. S29, *isomer* 1*a*) as the most likely substructure (99.97% confidence) (40). This result further verified by DP4+ (>99.99% confidence) after refining the NMR calculations at the PCM/mPW1PW91/6–31+G**//B3LYP/6–31G* level of theory (see *SI Appendix*, Tables S5 and S6 and accompanying diagrams) (41). From these summed experiments, petrichorin A was revealed to be a unique asymmetric dicyclohexapeptide, comprised of two distinct piperazyl cyclopeptides tethered by a biaryl linkage as shown in Fig. 1 (see *SI Appendix* for further data and detail).

Solving the molecular structure of petrichorin B was relatively straightforward compared to petrichorin A, owing to its symmetric, homodimeric structure. Following a similar battery of 1D and 2D NMR, hydrolytic component analysis, derivatization and theoretical NMR calculations used for petrichorin A (*SI Appendix*, Tables S3, S7, S8; Figs. S28, S33–S46) petrichorin B was found to consist of a symmetric homodimer of the same cyclopeptide that constitutes the left ring of petrichorin A (Fig. 1). While heterodimeric petrichorin A was unique in the chemical literature, petrichorin B was found to be highly similar to chloptosin (30). The only significant differences between them were that petrichorin B substitutes *allo*-isoleucine for chloptosin's valine, and petrichorin B has two γ-hydroxyl-piz moieties while all chloptosin piz residues are nonhydroxylated.

NRPS Assembly of the Petrichorins. The clear structural parallels that exist between petrichorin B and chloptosin suggested they likely arise from highly similar pathways, but the chloptosin BGC remains unreported in the literature, making it unavailable for comparison. While the *ltz* locus remains architecturally distinct in online sequence databases, published BGCs for the biosyntheses of the piperazyl cyclodepsipeptides himastatin and kutzneride from *Streptomyces himastatinicus* ATCC 53653 and *Kutzneria* sp. strain 744, respectively (*SI Appendix*, Fig. S47), share partial parallels with the *ltz* locus with regard to gene content and organization. However, the *ltz* locus critically lacks genes for the polyketide enzymology needed for depsipeptide linkages and their associated biosynthetic intermediates, which are integral to the kutznerides and himastatins.

The different peptide sequences making up each ring of the petrichorin A heterodimer (left ring: *D-allo*-ile, *L*-Piz, *D*-(*4S*-OH)-piz, *L-O*-methyl-ser, *D*-thr, *L*-6-Cl-HPIC; right ring: *D*-ala, *L*-piz, *D*-thr, *L-N*-methyl-ala, *D*-piz, *L*-7-Cl-HPIC) indicated each half of the molecule must be synthesized via distinct NRPS enzymology. Assigning which *ltz*-associated NRPS genes are responsible for petrichorin A and B biosyntheses initially involved bioinformatic analysis of the *ltz* cluster's NRPS enzymes to predict the order and chirality of possible peptide products

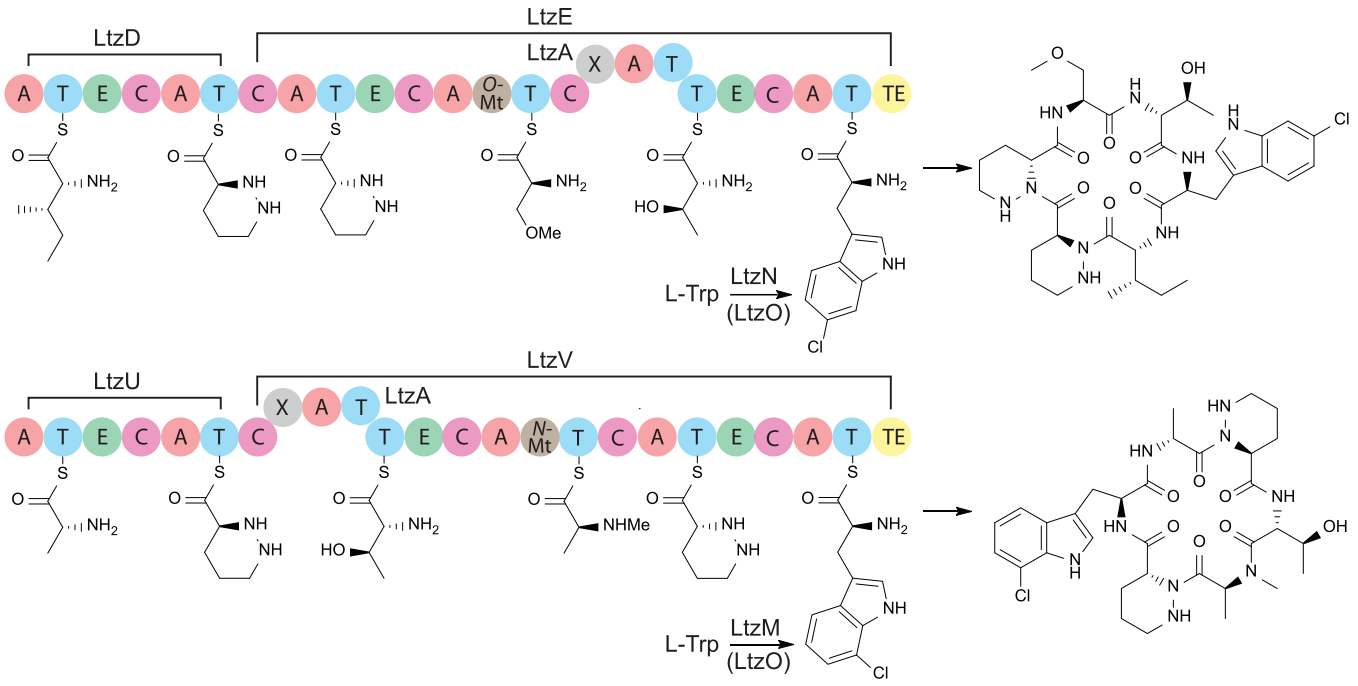

Fig. 3. Dual NRPS and flavin-dependent chlorinase assembly lines for the cyclopeptide precursors of petrichorin A and B. Note that cytochrome P450-dependent Piz-hydroxylation, HPIC-maturation, and aryl-crosslinking activities needed for precursor maturation and complete petrichorin assembly are excluded; see Figures 4 and 5. The predicted tryptophan chlorinase regiospecificites (LtzN, C6 and LtzM, C7; carbon assignment from 43) were inferred by protein identity against functionally characterized homologs (44, 45) (LtzN:Tar14, 66%; LtzM:PrnA, 59% identical). Flavin:nicotinamide cofactor oxidoreductases similar to LtzO often functionally pair with such enzymes. In both NRPS-assembly lines, LtzA is proposed to act *in trans* to compensate for absent adenylation domains in LtzV and LtzE. Standard NRPS domain abbreviations are used (A, adenylation; T, thiolation; E, epimerization; X, unknown function; *O*-Mt-, *O*-methyltransferase; *N*-Mt-, *N*-methyltransferase; TE, thioesterase).

(*SI Appendix*, Table S9). These data led us to posit that an NRPS assembly line consisting of LtzDE most likely directs the precursor of the left ring of petrichorin A (Figs. 1 and 3). Due to obvious structural parallels, this also implicates LtzDE in the production of homodimeric petrichorin B (Fig. 1). Concordantly, the assembly line comprised of LtzUV showed substantial collinearity with the expected peptide precursor of the right ring of petrichorin A. *O*-methyltransferase and *N*-methyltransferase domains found within NRPS proteins are readily discernable from each other by sequence (42), and single-instances of these domains were respectively found within LtzE and LtzV. Their placement within each NRPS assembly line dovetailed seamlessly with the rest of our molecular colinearity analyses. Finally, the presence of several epimerization domains within both NRPS assembly lines agreed with the actual structures of the petrichorins wherever *D*-configured amino acids were encountered (Fig. 3).

However, we noted both of the LtzDE and LtzUV assembly lines deviate from standard NRPS domain orders because each is missing a contextually expected adenylation domain (Fig. 3; LtzE module 3 and LtzV module 1). After comparing the domain orders of these assembly lines against the amino acids that comprise both petrichorins, the most parsimonious explanation is that LtzA (predicted to activate *L*-thr) must functionally replace both of these missing adenylation domains. Thus, LtzA likely acts as a transmodular NRPS enzyme, partnering with both LtzDE and LtzUV. While *trans*-acting NRPS adenylation modules remain fairly scarce in the literature, several examples are now documented (46). Furthermore, the kutzneride pathway requires one (47), and homology suggests one is likely to function in himastatin (31) production as well (HmtL module 6 is missing a necessary adenylation domain, and HmtF shares the same X-A-T domain order as LtzA).

To determine which NRPS assembly line(s) function in petrichorin A and B production, Δ*ltzU* and Δ*ltzD* mutations were created and the accumulation of piperazyl peptides were monitored by LC/MS/MS (Fig. 4). Deleting *ltzU* abrogated heterodimeric petrichorin A production, but not the homodimer petrichorin B, which agrees with precursor production model in Fig. 3. In contrast, deleting *ltzD* lost all dimeric cyclohexapeptide production. Instead, the strain accumulated a molecule with a mass consistent with a monomeric cyclopeptide. Once purified to homogeneity and structurally characterized (essentially as done for petrichorins A and B) (*SI Appendix*, Table S4 and Figs. S28, S48–S55), this biosynthetic intermediate (petrichorin C) was confirmed as being equivalent to one-half of the petrichorin A heterodimer (Fig. 1, legend). In addition, the simplified NMR spectra obtained for petrichorin C were used to further strengthen the initial NMR interpretations of the corresponding subregion of petrichorin A. We found it curious that we were unable to detect the theoretically possible dimer of petrichorin C in the *ltzD* mutant, while the homodimer petrichorin B was readily produced in the *ltzU* strain. The reason why the latter homodimer is readily produced while the other one apparently is not remains unknown.

Finally, the above analyses suggested that most of the biosynthetic building blocks required for NRPS-elaborated precursor peptide formation are either supplied via central metabolism through standard proteinogenic amino acid pools, or are produced by enzymes encoded within the cluster itself (i.e., piperazate, *ltzF*, and *ltzT*). The single exception to this was *L-allo*-ile, likely activated by LtzD module 1. *L-allo*-ile is known to be produced from *L*-ile in a pyridoxal phosphate-dependent, two-enzyme pathway that requires enzymes homologous to MfnO/DsdD and MfnH/DsaE (48). Missing from the *ltz* locus, searching the *L. flaviverrucosa* genome with MfnO and MfnH from the marformycin (49) cluster identified homologs (WP_090070987.1 and WP_090064152.1, respectively) encoded outside of the petrichorin supercluster that could potentially be involved in *allo*-ile production.

Cytochrome P450 Involvement in Petrichorin (Hetero)Dimer Formation and Tailoring. Multiple cytochrome P450 enzymes encoded within the chloptosin, himastatin, kutzneride, and alboflavusin biosynthetic loci are known to be involved in the maturation of tryptophan into HPIC (KtzM, HmtT, and AfnD), piperazyl peptide oxidation (HmtN and AfnA), and the formation of homodimeric (chloro)biaryl crosslinkages between HPIC residues (HmtS and ClpS) (30–32, 47, 50). While these transformations have been investigated elsewhere, we probed the functions of their homologs encoded within the *ltz*-locus (LtzR, LtzS, and LtzH, respectively; Fig. 5) for multiple reasons. These include a general difficulty in predicting biosynthetic P450 functions from sequence similarity alone (51), and LtzR, LtzS and LtzH are all members of the same P450 family (CYP113, using CYPED) (52). Furthermore, *Lentzea* affords an interesting opportunity to study these P450s within the context of a seldom-studied rare actinomycete host. Finally, none of the other pathways yield heterodimeric products, necessitating further investigation.

While limited numbers of P450s sourced from characterized piperazyl-HPIC cyclopeptide BGCs are available for comparison, we employed a maximum-likelihood inferred phylogeny (Fig. 5*A*) of the proteins above and their *ltz*-locus encoded homologs to assess if an evolutionary approach might better guide functional prediction. We found P450s involved in HPIC formation (blue highlights), HPIC-biaryl crosslinking (red highlights) formed monophyletic groups, and LtzR and LtzS, respectively, cladded within those groups. However, LtzH formed a separate group with HmtN, a piperazyl-peptide hydroxyating P450 from the himastatin (31) pathway and these were polyphyletic with AfnA (a P450 thought to have a similar function as HmtN) (32). Together, this suggested that biaryl linking and HPIC forming P450s might be discernable using molecular phylogeny, but piz-cyclopeptide hydroxylating P450s may have complex ancestry that complicates in silico identification.

From this, we inferred that LtzR is likely involved in petrichorin HPIC formation, LtzS is required for cyclopeptide crosslinking, and LtzH is involved in piperazyl hydroxylation (by virtue of its similarity to HmtN and the presence of *D*-(4-OH)-Piz subunits in both petrichorins). After constructing unmarked deletion mutants in *ltzR*, *ltzS*, and *ltzH*, we found that each strain accumulated several biosynthetic intermediates having retention times and masses distinct from petrichorin A and B. In concert with the phylogenetic predictions and previous himastatin biosynthesis and engineered alboflavusin dimerization analyses, we predicted that a Δ*ltzR* strain should be unable to produce crosslinked intermediates based on the inability of the strain to produce HPIC (where intact HPIC is apparently necessary for downstream P450 crosslinking) (32). Our high-resolution MS and LC/MS/MS of the piperazyl intermediates accumulated in this mutant found molecules having mass formulae corresponding to expected precursors of the left and right sides of petrichorin A (ZR1 and ZR2, Fig. 5 *B* and *E*) which feature chloro-tryptophan residues in place of chloro-HPIC, in agreement with our predictions.

We found that deleting *ltzS* led to the production of petrichorin C, which was initially discovered in this work after accumulating in our Δ*ltzD* NRPS mutant (Fig. 4). In contrast with the *ltzD* mutant (unable to synthesize the left cyclopeptide chain of petrichorin A and the entirety of petrichorin B), mutating *ltzS* led to concomitant accumulation of an additional molecule (ZS2) having a mass formula equivalent to the predicted left cyclohexapeptide of the petrichorin A dimer (Fig. 5 *C* and *F*). Accordingly, ZS2 was then also posited to be

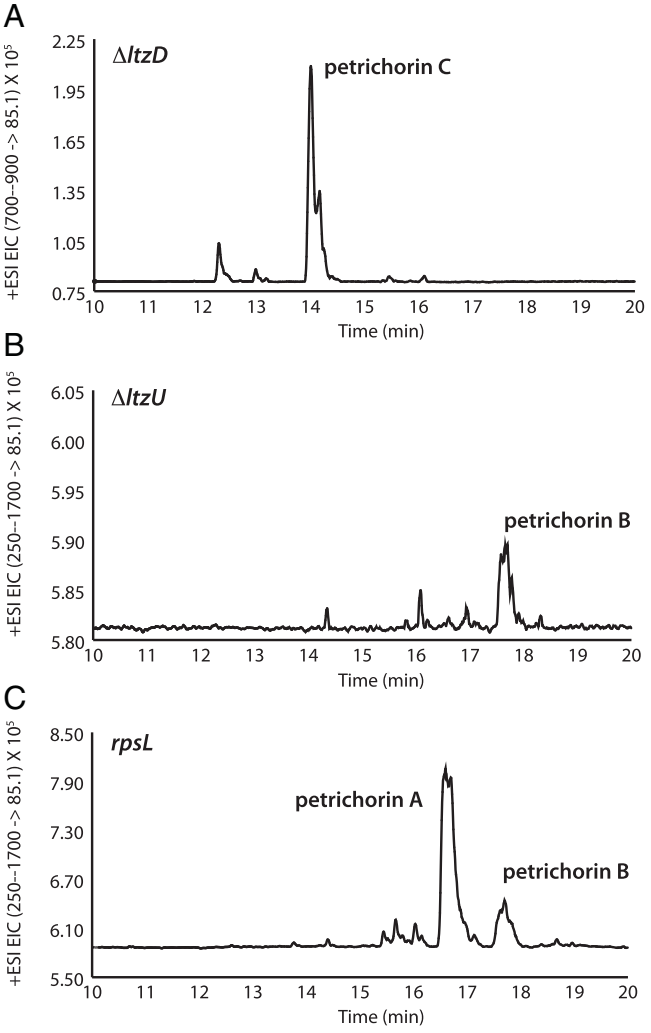

Fig. 4. Biosynthetic analysis of petrichorin NRPS gene mutants *ltzD* and *ltzU* via LC/MS/MS. (*A*) Deleting *ltzD* caused the loss of petrichorin A and B, with the concomitant accumulation of the monomer petrichorin C. In contrast, deleting (*B*) *ltzU* abrogated only petrichorin A, while the homodimer petrichorin B continued production. Thus, *ltzU* is essential for petrichorin A production via the petrichorin C intermediate, while *ltzD* is responsible for the cyclopeptide intermediate that is matured into petrichorin B, plus one-half of the petrichorin A heterodimer. (*C*) *rpsL* parental control showing the relative retention times of petrichorin A and B.

structurally equivalent to the cyclopeptide monomer that is dimerized to create petrichorin B. Finally, deleting *ltzH* led to the production of biosynthetic intermediates with masses that correspond to petrichorin A missing a lone piz-hydroxyl group, or petrichorin B lacking both piz-hydroxyl decorations (Fig. 5 *D* and *G*; ZH1 and ZH2 respectively, where ZH2 is potentially identical to chloptosin C) (53). Importantly, all of these P450 were genetically complemented to restore petrichorin A and B, indicating the accumulated intermediates were not influenced by transcriptional polarity (*SI Appendix*, Fig. S56). Taken together, these data offer strong evidence for *ltz*-locus P450 function that is congruent with our phylogenetic analysis.

Analysis of Petrichorin Regulation. Many actinomycete BGCs encode for cluster-situated regulators (CSRs), proteins that function to coordinate transcriptional regulation of the genes in their cluster neighborhood (55). The BGCs encoding for himastatin and the kutznerides both encode CSRs (31, 47), but appear to employ dissimilar regulatory strategies based on a lack of contextually conserved regulatory proteins between

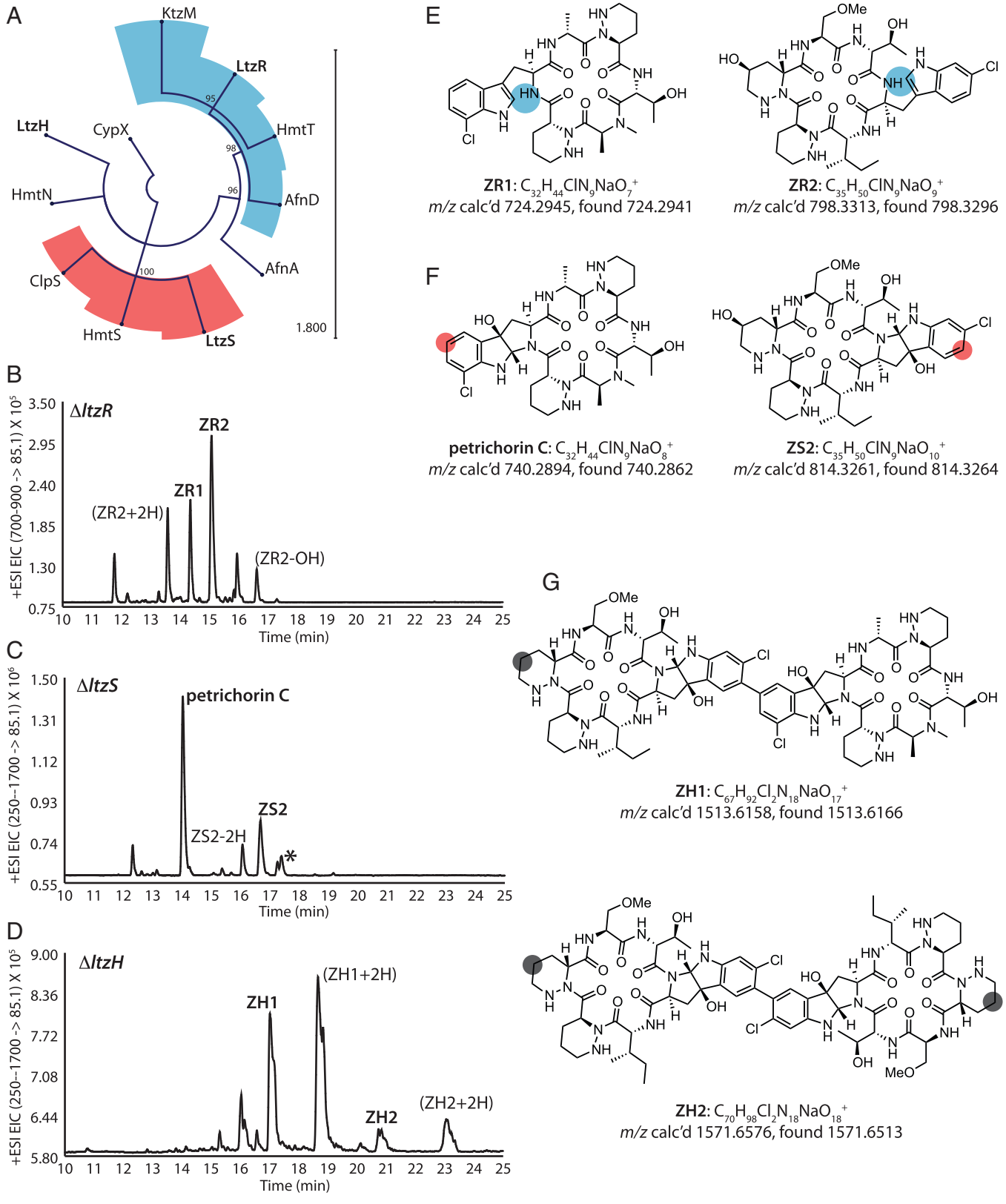

Fig. 5. Phylogenetic and metabolic analyses to assign *ltz*-locus cytochrome P450 gene functions. The cytochrome P450s associated with BGCs encoding molecules like those found in Fig. 1 share significant homology and are thus challenging to functionally assign via sequence identity alone (32). However, (*A*) a maximum-likelihood phylogeny bins P450s involved in HPIC maturation (blue branches) and biaryl-crosslinking (red branches) into monophyletic groups, indicating potential orthology. In contrast, putative piperazyl-hydroxylating P450s (HmtN, LtzH and AfnA) failed to show similar monophyly. CypX (AGS49593.1) (54), an exemplar CYP113C-family P450, was used as an outgroup; the tree was constructed with 500 bootstraps and branches <90% confidence were collapsed with actual values noted at nodes. (*B–D*) LC/MS/MS analysis of biosynthetic intermediates accumulated in *ltzR*, *ltzS*, and *ltzH* mutants, respectively, plus (*E–G*) homology-inferred and HRMS-supported structures of key molecules arising in each mutant. For each proposed intermediate, the shaded circles indicate the target of each P450, with colors matching those used to highlight the tree in (*A*). Hydroxylation targets are indicated in dark charcoal (*G*). Several mutants accumulated intermediates having masses commensurate with hydride [2H] or hydroxyl [OH] additions or losses (±) to the illustrated structures; these are denoted within chromatogram peak callouts for clarity. Peak in (*C*) indicated with * has a mass equivalent with ZS2; indicating a likely geometric isomer thereof.

Table 1. Petrichorin IC_{50} values (nM) against select human cancer cell lines with paclitaxel control

Cell lines	Petrichorin A	Petrichorin B	Petrichorin C	Paclitaxel
A2780	28.12 ± 2.329	35.32 ± 4.289	169.14 ± 2.860	8.127 ± 2.156
HT1080	35.51 ± 4.194	36.36 ± 3.423	72.41 ± 3.021	75.0 ± 2.511
PC3	34.49 ± 2.262	68.43 ± 3.296	273.46 ± 3.385	136.0 ± 1.494
Jurkat	20.25 ± 2.624	72.47 ± 1.551	101.9 ± 3.014	8.694 ± 2.699

them. Xie et al. (56) found that himastain biosynthetic regulation is complex, suggesting two canonical transcriptional regulators encoded within the compound's BGC (HmtA and HmtD) are chiefly involved. These proteins respectively belong to the MerR and ParB regulatory families, which contrasts with the single SARP-family transcriptional regulator (KtzK) encoded within the core of the kutzeride BGC. Comparing the *ltz* locus against these clusters revealed a single SARP-encoding gene (*ltzP*), suggesting closer regulatory parallels with the kutzneride locus. While kutzneride regulation remains experimentally uncharacterized, deleting *ltzP* led to the complete loss of petrichorin production (JV755) (*SI Appendix*, Fig. S57), as well as any LC/MS/MS detectable piperazyl intermediates, supporting the idea that LtzP encodes for an essential petrichorin regulator. The mutant was rescued by *ltzP* ectopic expression (JV825), but not kutzneride homolog *ktzK* (JV826), suggesting these regulators have host-specific functions, possibly stemming from different regulator-DNA sequence tropisms.

Himastatin regulatory analyses also suggested that *hmtB*, encoding an acetylglutamate kinase type protein may act as a metabolic regulator (56). While the *ltz* locus lacks a homolog of this protein, we found that deleting *ltzB* (encoding a protein similar to acyl-CoA oxidoreductases) led to the complete abrogation of petrichorin production and any detectable intermediates (*SI Appendix*, Fig. S57). Similar to the *ltzP* regulatory phenotype above, this suggested the *ltz* locus may also employ metabolic regulatory mechanisms (similar to that inferred for *hmtB*). Ectopic expression of *ltzB* weakly rescued the Δ*ltzB* phenotype, indicating that polarity is not likely causal (*SI Appendix*, Fig. S57).

Interestingly, Ma et al. (31) found that deleting the *ltzB* homolog encoded within the himastatin locus (*hmtG*) led to complete compound loss, leading those authors to speculate that *hmtG* may be involved in piz production. Because piz biosynthesis is now solved, this explanation seems less likely. However, the strong phenotypes accompanying LtzB/HmtG loss indicates a critical role must exist. Interestingly, both proteins are encoded within syntenic cassettes, characterized an NRPS gene encoding a predicted X-A-T domain arrangement (*ltzA/hmtF*), an acyl-CoA oxidoreductase (*ltzB/hmtG*), then a type II thioesterase (*ltzC/hmtH*). This conserved arrangement, in combination with our proposed functions for LtzA, led us to infer that LtzB/HmtG proteins may be involved in modulating NRPS protein-protein interactions or a related role. How the oxidoreductase functionality of these proteins might integrate into such a system also needs investigation, but *trans*-acting proteins are widely known to modulate NRPS assembly lines, including MbtH-type proteins (57) (encoded by *ltzG* in the petrichorin locus).

Petrichorin Cytotoxicity Assays. The dimeric cyclo(depsi)peptides chloptosin, himastatin, and enzymatically cross-linked alboflavusins show compelling cytotoxicity profiles (30, 32, 58), and their structural parallels with the petrichorins suggested the latter compounds may have similar properties. Thus, petrichorin A was evaluated for anti-proliferative activity against multiple cancer cell lines. Naturally heterodimeric petrichorin A was active against A2780 human ovarian cancer, HT1080 fibrosarcoma, the PC3 human prostate cancer, and the Jurkat human T lymphocyte cell lines (a model for acute T cell leukemia) with IC_{50} values in the range of 20–36 nM. Petrichorins B and C were also active, but to a generally lower extent than petrichorin A. Homodimeric petrichorin B inhibited the four cell lines with IC_{50} values of 35–73 nM, while monomeric petrichorin C was the least active with IC_{50} values ranging from 73–274 nM (versus paclitaxel control, Table 1 and *SI Appendix*, Fig. S58). Prior alboflavusin monomer vs. dimer structure-activity studies (32) led us to predict that monomeric petrichorin C would likely be less active than dimeric petrichorins A and B. However, because homodimers are far more common versus heterodimeric compounds in the context of polyvalent drug development (59), observing that petrichorin A is generally more active than petrichorin B was somewhat surprising. This suggests aryl-crosslinked cyclopeptide heterodimers like petrichorin A, whether encoded by nature or synthesized in a directed way, should be closely considered for future polyvalent molecular diversification and design.

Conclusions

Actinomycetes are a valued source of biologically active compounds. However, there is a recognized historical bias in how these organisms have been prosecuted for pharmaceutical discovery, with infrequently encountered "rare actinomycetes" remaining less-explored. The problem of molecule rediscovery is one of several significant reasons quoted to explain why large pharmaceutical companies mostly withdrew from actinomycete-based drug discovery programs (7). However, facing a broadly recognized need for new anti-infectives and other drugs, rare actinomycetes remain relatively fertile for the discovery of novel medicines (24). Despite their perceived value, the biotechnological exploitation of rare actinomycetes can be challenging. Compared to more common *Streptomyces*, are fewer rare actinomycetes in cultivation and they often suffer from less-developed genetic toolsets for genome engineering and other important manipulations.

In an effort to discover new bioactive compounds from rare actinomycetes, we designed and tested a bottom-up discovery approach for the targeted metabologenomic identification of yet- undiscovered piperazyl natural products produced by *L. flaviverrucosa*. The recent discovery of the *Streptomyces* incarnatapeptin piperazyl-peptides via a combined *pzbB* mining–^{15}N NMR discovery program (60) demonstrates the power of metabologenomics for targeted piperazyl molecule discovery. This work adds to prior efforts by devising a high-throughput adaptable MS/MS-based approach in place of NMR as a primary screening tool, while also demonstrating that often-used *Streptomyces* genetic toolsets are transferrable to *L. flaviverrucosa*.

Biosynthetic superclusters are chromosomally adjacent biosynthetic loci that often direct the production of synergistic pairs of molecules. This synergy results in complex pathway inhibition and robust bioactivity profiles for producing organisms (for a recent review, see 61). Here, the main product of petrichorin

supercluster (petrichorin A) is a pair structurally distinct cyclopeptides that are crosslinked by cytochrome P450 LtzS. LtzS is apparently versatile; being essential for heterodimeric petrichorin A but it also catalyzes minor homodimeric (petrichorin B) chloro-biaryl cyclopeptde crosslinking. While Guo et al. (32) recently reported the use of related P450s for homodimeric HPIC-piperazyl cyclopeptide crosslinking to bioengineer new cytotoxic homodimers, our findings now highlight enzymes within the LtzS/ClpS/HmtS clade for (chloro)biaryl- heterodimer catalysis as well. This suggests additional clade-members could be sought for diversifying HPIC-cyclopeptides via heteromulitimerization.

Several mechanisms are suggested to explain why polyvalent molecules, often symmetric homodimers or higher-order multimers, have superior biological activities against monomeric analogs (59, 62–64). Given this, the substantive bioactivity activity seen for bilaterally asymmetric petrichorin A (especially in comparison to symmetric petrichorin B) is intriguing and should inspire future heterodimer structure-activity relationship and mechanistic research against additional cell lines and organisms. In sum, this study provides a framework for the exploration and directed biosynthesis of asymmetric cyclopeptide heterodimers, illustrates the utility of a mass-spectrometric-based metabologenomics approach for desirable piperazates, and highlights *L. flaviverrucosa* as a rare actinomycete amenable to manipulation for biotechnological development.

Materials and Methods

Materials. All standard laboratory chemicals were purchased from Sigma-Aldrich, Fisher Scientific, or Santa Cruz Biotechnology. Microbiological media ingredients were purchased from DIFCO. d^7-*L*-ornithine was purchased from C/D/N Isotopes and *L*-piperazic acid dihydrochloride was synthesized and purchased from WuXi AppTec. The publicly available genome sequence of *L. flaviverrucosa* (GenBank PRJNA463399) was used to guide these studies (*ltzA-ltzU*; RDI25332.1–RDI25353.1, respectively). See *SI Appendix*, Table S10 for the oligonucleotides used in this study.

Growth and Strains. *Lentzea flaviverrucosa* DSM 44664 was routinely propagated on ISP2 agar (International *Streptomyces* Project Medium 2, Difco) and TSB (Trypticase Soy Broth, Difco) at 28 °C. Colony PCR templates were prepared by grinding a colony in 100 μL DMSO, essentially as noted elsewhere (65). *Escherichia coli* was routinely propagated on lysogeny broth Agar and broth at 37 °C according to standard methods. *SI Appendix* and Tables S11 and S12 list plasmids and strains used in this work. For details on intergenic conjugation, and deletion mutant construction, and bioactivity assays (essentially as in 66–71), see the *SI Appendix*.

Petrichorin Detection. *Lentzea flaviverrucosa* colonies were used to inoculate 15 mL of TSB liquid media in a 125-mL Erlenmeyer flask equipped with 6-mm glass beads and vigorous shaking at 28 °C. After 2 d of growth, the culture was plated on ATCC172 (American Type Culture Collection Medium 172) and incubated at 28 °C for 4 d. During initial petrichorin discovery, SMMS agar (72) was also used to afford a less complex LC/MS background signal. After growth, solid agar with adherent cells was chopped into pieces and immersed in ethyl acetate overnight. The resulting extract was evaporated under vacuum and the extract was suspended in 500 μL of HPLC-grade methanol. Methanolic suspensions were syringe-filtered (Agilent Captiva Econo Filter, 0.2 μL) before LC/MS analysis. This was performed using a Phenomenex Luna C18 column (75 × 3 mm, 3 μm pore size) installed on an Agilent 1260 Infinity HPLC connected in-line to an Agilent 6420 Triple-Quad mass spectrometer using the following method: $T = 0$, 10% B; $T = 5$, 10% B; $T = 25$, 100% B; $T = 27$, 100% B; $T = 29$, 10% B; $T = 30$, 10% B; A: water + 0.1% formic acid; and B: acetonitrile + 0.1% formic acid; 0.6 mL/min. Ten microliters of the methanol-dissolved extract was injected per run, and a total ion count chromatogram was obtained for each sample. Electrospray ionization was used, with MS/MS collision voltage set to 80 V for cyclic petrichorins with product ion scanning as noted in text. Mass filtering between *m/z* 1300–1700 was used to detect intact petrichorin congeners; lower mass bounds were utilized when analyzing biosynthetic intermediates to reduce background signals. For *L*-piz labeling, a stock solution of 25 mg/mL L-piperazic acid•2HCl was filter sterilized and diluted to the desired concentrations with purified water. Two hundred microliters of the working stock was spread on each ATCC172 plate and allowed to dry before 200 μL of overnight *L. flaviverrucosa* cultures were spread. The calculated concentrations used in agar plates were 10, 50, 100, 500, and 1000 μM. The plates were incubated at 28 °C for 4 d, then the agar with cells was extracted with ethyl acetate overnight. The ethyl acetate was evaporated under vacuum and crude extracts were resuspended in 500 μL methanol and syringe-filtered before analysis.

General Chemistry. Optical rotations were measured with a Rudolph Research Analytical Autopal IV Automatic polarimeter. Ultraviolet and infrared spectra were obtained with Shimadzu UV-1800 spectrophotometer and ThermoScientific Nicolet iS50FT-IR spectrometer, respectively. NMR spectra were recorded in Acetone-d_6 with 2 drops of DMSO-d_6 on Varian Unity Inova 500 MHz and Bruker 400 MHz; high resolution mass spectra were obtained an Agilent Q-TOF Ultima ESI-TOF mass spectrometer. Preparative HPLC was carried out on a ThermoScientific U3000 LC system. Extensive multidimensional NMR supporting data are found in the *SI Appendix*.

Isolation of Compounds Petrichorins A–C. *Lentzea flaviverrucosa* DSM 44664 was cultured on ATCC172 agar plates at 28 °C for 5 d. The ethyl acetate (EtOAc) crude extract (1.41 g) was subjected to preparative HPLC (phenyl-hexyl column, 5 μm; 100.0 × 21.2 mm; 10 mL/min; with 0.1% formic acid in mobile phases) eluted with 20–100% acetonitrile/H_2O in 40 min to obtain 40 fractions (SF.1–40). F17 (57.2 mg) and F18 (32.8 mg) were further separated by semipreparative HPLC (C18 column, 5 μm; 250.0 mm × 10.0 mm; 4 mL/min; with 0.1% formic acid in 78% CH_3OH/H_2O) to yield petrichorin A (35.7 mg, t_R 11.4 min) and petrichorin B (3.61 mg, t_R 14.7 min), respectively. Mutant strain JV757 (Δ*ltzD*) was also cultured on 5 L equivalent of ATCC172 media agar plates at 28 °C for 6 d. The EtOAc crude extract (471.28 mg) was subjected to preparative HPLC (phenyl-hexyl column, 5 μm; 100.0 × 21.2 mm; 10 mL/min; with 0.1% formic acid in mobile phases) eluted with 20–100% methanol/H_2O in 35 min to get 35 fractions (F1-35). All the fractions were analyzed by LC/MS and the target compound with the molecule weight of 717 Da was detected in F28. Further separation of F28 (9.68 mg) with semipreparative HPLC (C18 column, 5 μm; 250.0 mm × 10.0 mm; 4 mL/min; 20–40% CH_3CN/H_2O in 60 min) led to the isolation of petrichorin C (3.25 mg, t_R 28.5 min). Details on the hydrolysis and analysis of the petrichorins via Marfey (*SI Appendix*, Table S13) and Mosher derivatization (essentially as previously described) (37, 38) are in the SI Appendix. Also see *SI Appendix* for details of DP4 NMR calculations (73).

Data Availability. All study data are included in the article and/or *SI Appendix*.

ACKNOWLEDGMENTS. The authors thank Lee Douangkeomany for assistance with *Lentzea* mutagenesis. This work was supported by the Hawaii Community Foundation (15ADVC-74420, 17CON-86295, and 20CON-102163), and the Hawaii IDeA Network for Biomedical Research Excellence III and IV (INBRE-III and INBRE-IV) project (NIGMS grant 5P20GM103466) to S.C. This work was also supported by NSF-CAREER 1846005 to J.A.V.B.

Author affiliations: [a]Department of Pharmaceutical Sciences, Daniel K. Inouye College of Pharmacy, University of Hawaii at Hilo, Hilo, HI 96720; [b]Cancer Biology Program, University of Hawaii Cancer Center, Honolulu, HI 96813; [c]Department of Biology, Washington University in St Louis, St Louis MO 63122; and [d]Instituto de Química Rosario (CONICET), Facultad de Ciencias Bioquímicas y Farmacéuticas, Universidad Nacional de Rosario, Rosario 2000, Argentina

Author contributions: C.L., Y.H., A.M.S., S.C., and J.A.V.B. designed research; C.L., Y.H., X.W., S.D.S., Y.Q., J.M.D., K.K.N., and A.M.S. performed research; C.L., Y.H., X.W., S.D.S., Y.Q., J.M.D., K.K.N., A.M.S., S.C., and J.A.V.B. analyzed data; and S.C. and J.A.V.B. wrote the paper.

[1]C.L. and Y.H. contributed equally to this work.

[2]Present address: Antheia, Inc., Menlo Park, CA 94025.

[3]Present address: Pritzker School of Medicine, The University of Chicago, Chicago, IL 60637.

[4]Present address: Pfizer Inc, Chesterfield, MO 63017.

[5]Present address: Animal Sciences Research Center, University of Missouri, Columbia, MO 65211.

1. A. T. Bull, A. C. Ward, M. Goodfellow, Search and discovery strategies for biotechnology: The paradigm shift. *Microbiol. Mol. Biol. Rev.* **64**, 573–606 (2000).
2. M. I. Hutchings, A. W. Truman, B. Wilkinson, Antibiotics: Past, present and future. *Curr. Opin. Microbiol.* **51**, 72–80 (2019).
3. R. H. Baltz, Renaissance in antibacterial discovery from actinomycetes. *Curr. Opin. Pharmacol.* **8**, 557–563 (2008).
4. A. G. Atanasov, S. B. Zotchev, V. M. Dirsch, C. T. Supuran; International Natural Product Sciences Taskforce, Natural products in drug discovery: Advances and opportunities. *Nat. Rev. Drug Discov.* **20**, 200–216 (2021).
5. M. L. Cohen, Changing patterns of infectious disease. *Nature* **406**, 762–767 (2000).
6. L. Katz, R. H. Baltz, Natural product discovery: Past, present, and future. *J. Ind. Microbiol. Biotechnol.* **43**, 155–176 (2016).
7. R. H. Baltz, Genome mining for drug discovery: Progress at the front end. *J. Ind. Microbiol. Biotechnol.* **48**, kuab044 (2021).
8. B. O. Bachmann, S. G. Van Lanen, R. H. Baltz, Microbial genome mining for accelerated natural products discovery: Is a renaissance in the making? *J. Ind. Microbiol. Biotechnol.* **41**, 175–184 (2014).
9. D. W. Udwary, H. Otani, N. J. Mouncey, New keys to unlock the treasure trove of microbial natural products. *Nat. Rev. Microbiol.* **19**, 683 (2021).
10. P. A. Hoskisson, R. F. Seipke, Cryptic or silent? The known unknowns, unknown knowns, and unknown unknowns of secondary metabolism. *MBio* **11**, e02642–e02620 (2020).
11. J.-L. Wolfender, M. Litaudon, D. Touboul, E. F. Queiroz, Innovative omics-based approaches for prioritisation and targeted isolation of natural products - new strategies for drug discovery. *Nat. Prod. Rep.* **36**, 855–868 (2019).
12. O. N. Sekurova, O. Schneider, S. B. Zotchev, Novel bioactive natural products from bacteria via bioprospecting, genome mining and metabolic engineering. *Microb. Biotechnol.* **12**, 828–844 (2019).
13. M. A. Ciufolini, N. Xi, Synthesis, chemistry and conformational properties of piperazic acids. *Chem. Soc. Rev.* **27**, 437–439 (1998).
14. M. E. Welsch, S. A. Snyder, B. R. Stockwell, Privileged scaffolds for library design and drug discovery. *Curr. Opin. Chem. Biol.* **14**, 347–361 (2010).
15. E. L. Handy, J. K. Sello, "Structure and synthesis of conformationally constrained molecules containing piperazic acid" in *Peptidomimetics I. Topics in Heterocyclic Chemistry*, W.. Lubell, Eds., (Springer, 2015), **vol. 48**, pp. 97–124.
16. W. Jiang *et al.*, Biosynthetic chlorination of the piperazate residue in kutzneride biosynthesis by KthP. *Biochemistry* **50**, 6063–6072 (2011).
17. Y.-L. Du, H.-Y. He, M. A. Higgins, K. S. Ryan, A heme-dependent enzyme forms the nitrogen-nitrogen bond in piperazate. *Nat. Chem. Biol.* **13**, 836–838 (2017).
18. Y. Hu, Y. Qi, S. D. Stumpf, J. M. D'Alessandro, J. A. V. Blodgett, Bioinformatic and functional evaluation of actinobacterial piperazate metabolism. *ACS Chem. Biol.* **14**, 696–703 (2019).
19. C. S. Sit *et al.*, Variable genetic architectures produce virtually identical molecules in bacterial symbionts of fungus-growing ants. *Proc. Natl. Acad. Sci. U.S.A.* **112**, 13150–13154 (2015).
20. D.-C. Oh, M. Poulsen, C. R. Currie, J. Clardy, Dentigerumycin: A bacterial mediator of an ant-fungus symbiosis. *Nat. Chem. Biol.* **5**, 391–393 (2009).
21. D. Shin *et al.*, Coculture of marine *Streptomyces* sp. with *Bacillus* sp. produces a new piperazic acid-bearing cyclic peptide. *Front Chem.* **6**, 498 (2018).
22. K. D. Morgan, R. J. Andersen, K. S. Ryan, Piperazic acid-containing natural products: Structures and biosynthesis. *Nat. Prod. Rep.* **36**, 1628–1653 (2019).
23. M. Goodfellow, I. Nouioui, R. Sanderson, F. Xie, A. T. Bull, Rare taxa and dark microbial matter: Novel bioactive actinobacteria abound in Atacama Desert soils. *Antonie van Leeuwenhoek* **111**, 1315–1332 (2018).
24. K. Tiwari, R. K. Gupta, Rare actinomycetes: A potential storehouse for novel antibiotics. *Crit. Rev. Biotechnol.* **32**, 108–132 (2012).
25. K. Pommerehne, J. Walisko, A. Ebersbach, R. Krull, The antitumor antibiotic rebeccamycin-challenges and advanced approaches in production processes. *Appl. Microbiol. Biotechnol.* **103**, 3627–3636 (2019).
26. H. Lee, J.-W. Suh, Anti-tuberculosis lead molecules from natural products targeting *Mycobacterium tuberculosis* ClpC1. *J. Ind. Microbiol. Biotechnol.* **43**, 205–212 (2016).
27. D. Wichner *et al.*, Isolation and anti-HIV-1 integrase activity of lentzeosides A-F from extremotolerant *Ientzea* sp. H45, a strain isolated from a high-altitude Atacama Desert soil. *J. Antibiot. (Tokyo)* **70**, 448–453 (2017).
28. S. Sasamura *et al.*, Bioconversion of FR901459, a novel derivative of cyclosporin A, by *Lentzea* sp. 7887. *J. Antibiot. (Tokyo)* **68**, 511–520 (2015).
29. W. Tao *et al.*, A genomics-led approach to deciphering the mechanism of thiotetronate antibiotic biosynthesis. *Chem. Sci. (Camb.)* **7**, 376–385 (2016).
30. K. Umezawa, Y. Ikeda, Y. Uchihata, H. Naganawa, S. Kondo, Chloptosin, an apoptosis-inducing dimeric cyclohexapeptide produced by *Streptomyces*. *J. Org. Chem.* **65**, 459–463 (2000).
31. J. Ma *et al.*, Biosynthesis of himastatin: Assembly line and characterization of three cytochrome P450 enzymes involved in the post-tailoring oxidative steps. *Angew. Chem. Int. Ed. Engl.* **50**, 7797–7802 (2011).
32. Z. Guo *et al.*, Design and biosynthesis of dimeric alboflavusins with biaryl linkages via regiospecific C–C bond coupling. *J. Am. Chem. Soc.* **140**, 18009–18015 (2018).
33. Z. Guo *et al.*, NW-G01, a novel cyclic hexapeptide antibiotic, produced by *Streptomyces alboflavus* 313: II. Structural elucidation. *J. Antibiot. (Tokyo)* **63**, 231–235 (2010).
34. A. Broberg, A. Menkis, R. Vasiliauskas, Kutznerides 1-4, depsipeptides from the actinomycete *Kutzneria* sp. 744 inhabiting mycorrhizal roots of *Picea abies* seedlings. *J. Nat. Prod.* **69**, 97–102 (2006).
35. T. Ogita *et al.*, Matlystatins, new inhibitors of typeIV collagenases from *Actinomadura atramentaria*. I. Taxonomy, fermentation, isolation, and physico-chemical properties of matlystatin-group compounds. *J. Antibiot. (Tokyo)* **45**, 1723–1732 (1992).
36. F. Leipoldt *et al.*, Warhead biosynthesis and the origin of structural diversity in hydroxamate metalloproteinase inhibitors. *Nat. Commun.* **8**, 1965 (2017).
37. K. C.-C. Cheng *et al.*, Actinoramide A identified as a potent antimalarial from titration-based screening of marine natural product extracts. *J. Nat. Prod.* **78**, 2411–2422 (2015).
38. S. Cao *et al.*, Ipomoeassins A-E, cytotoxic macrocyclic glycoresins from the leaves of *Ipomoea squamosa* from the Suriname rainforest. *J. Nat. Prod.* **68**, 487–492 (2005).
39. N. Grimblat, A. M. Sarotti, Computational chemistry to the rescue: Modern toolboxes for the assignment of complex molecules by GIAO NMR calculations. *Chemistry* **22**, 12246–12261 (2016).
40. N. Grimblat, J. A. Gavín, A. Hernández Daranas, A. M. Sarotti, Combining the power of J coupling and DP4 analysis on stereochemical assignments: The J-DP4 methods. *Org. Lett.* **21**, 4003–4007 (2019).
41. N. Grimblat, M. M. Zanardi, A. M. Sarotti, Beyond DP4: An improved probability for the stereochemical assignment of isomeric compounds using quantum chemical calculations of NMR shifts. *J. Org. Chem.* **80**, 12526–12534 (2015).
42. T. A. Lundy, S. Mori, S. Garneau-Tsodikova, A thorough analysis and categorization of bacterial interrupted adenylation domains, including previously unidentified families. *RSC Chem Biol* **1**, 233–250 (2020).
43. L. M. Alkhalaf, K. S. Ryan, Biosynthetic manipulation of tryptophan in bacteria: Pathways and mechanisms. *Chem. Biol.* **22**, 317–328 (2015).
44. H. Luhavaya, R. Sigrist, J. R. Chekan, S. M. K. McKinnie, B. S. Moore, Biosynthesis of l-4-chlorokynurenine, an antidepressant prodrug and a non-proteinogenic amino acid found in lipopeptide antibiotics. *Angew. Chem. Int. Ed. Engl.* **58**, 8394–8399 (2019).
45. C. Dong *et al.*, Tryptophan 7-halogenase (PrnA) structure suggests a mechanism for regioselective chlorination. *Science* **309**, 2216–2219 (2005).
46. M. Bernhardt, S. Berman, D. Zechel, A. Bechthold, Role of Two Exceptional trans Adenylation Domains and MbtH-like Proteins in the Biosynthesis of the Nonribosomal Peptide WS9324A from *Streptomyces calvus* ATCC 13382. *ChemBioChem* **21**, 2659–2666 (2020).
47. D. G. Fujimori *et al.*, Cloning and characterization of the biosynthetic gene cluster for kutznerides. *Proc. Natl. Acad. Sci. U.S.A.* **104**, 16498–16503 (2007).
48. Q. Li *et al.*, Deciphering the biosynthetic origin of L-*allo*-isoleucine. *J. Am. Chem. Soc.* **138**, 408–415 (2016).
49. J. Liu *et al.*, Biosynthesis of the anti-infective marformycins featuring pre-NRPS assembly line *N*-formylation and *O*-methylation and post-assembly line C-hydroxylation chemistries. *Org. Lett.* **17**, 1509–1512 (2015).
50. P. Ruiz-Sanchis, S. A. Savina, F. Albericio, M. Álvarez, Structure, bioactivity and synthesis of natural products with hexahydropyrrolo[2,3-b]indole. *Chemistry* **17**, 1388–1408 (2011).
51. J. D. Rudolf, C.-Y. Chang, M. Ma, B. Shen, Cytochromes P450 for natural product biosynthesis in *Streptomyces*: Sequence, structure, and function. *Nat. Prod. Rep.* **34**, 1141–1172 (2017).
52. D. Sirim, F. Wagner, A. Lisitsa, J. Pleiss, The cytochrome P450 engineering database: Integration of biochemical properties. *BMC Biochem.* **10**, 27 (2009).
53. H. Hashizume *et al.*, New chloptosins B and C from an *Embleya* strain exhibit synergistic activity against methicillin-resistant *Staphylococcus aureus* when combined with co-producing compound L-156,602. *J. Antibiot. (Tokyo)* **74**, 80–85 (2021).
54. J. G. Owen *et al.*, Mapping gene clusters within arrayed metagenomic libraries to expand the structural diversity of biomedically relevant natural products. *Proc. Natl. Acad. Sci. U.S.A.* **110**, 11797–11802 (2013).
55. G. Liu, K. F. Chater, G. Chandra, G. Niu, H. Tan, Molecular regulation of antibiotic biosynthesis in *streptomyces*. *Microbiol. Mol. Biol. Rev.* **77**, 112–143 (2013).
56. Y. Xie, Q. Li, X. Qin, J. Ju, J. Ma, Enhancement of himastatin bioproduction via inactivation of atypical repressors in *Streptomyces hygroscopicus*. *Metab. Eng. Commun.* **8**, e00084 (2019).
57. E. A. Felnagle *et al.*, MbtH-like proteins as integral components of bacterial nonribosomal peptide synthetases. *Biochemistry* **49**, 8815–8817 (2010).
58. K. S. Lam *et al.*, Himastatin, a new antitumor antibiotic from *Streptomyces hygroscopicus*. I. Taxonomy of producing organism, fermentation and biological activity. *J. Antibiot. (Tokyo)* **43**, 956–960 (1990).
59. A. Greer, O. R. Wauchope, N. S. Farina, P. Haberfield, J. F. Liebman, Paradigms and paradoxes: Mechanisms for possible enhanced biological activity of bilaterally symmetrical chemicals. *Struct. Chem.* **17**, 347–350 (2006).
60. K. D. Morgan *et al.*, Incarnatapeptins A and B, Nonribosomal Peptides Discovered Using Genome Mining and $^{1}H/^{15}N$ HSQC-TOCSY. *Org. Lett.* **22**, 4053–4057 (2020).
61. K. J. Meyer, J. R. Nodwell, Biology and applications of co-produced, synergistic antimicrobials from environmental bacteria. *Nat. Microbiol.* **6**, 1118–1128 (2021).
62. H. Aldemir, R. Richarz, T. A. Gulder, The biocatalytic repertoire of natural biaryl formation. *Angew. Chem. Int. Ed. Engl.* **53**, 8286–8293 (2014).
63. C. Chittasupho, Multivalent ligand: Design principle for targeted therapeutic delivery approach. *Ther. Deliv.* **3**, 1171–1187 (2012).
64. J. H. Griffin *et al.*, Multivalent drug design. Synthesis and in vitro analysis of an array of vancomycin dimers. *J. Am. Chem. Soc.* **125**, 6517–6531 (2003).
65. W. Van Dessel, L. Van Mellaert, N. Geukens, J. Anné, Improved PCR-based method for the direct screening of *Streptomyces* transformants. *J. Microbiol. Methods* **53**, 401–403 (2003).
66. J. A. V. Blodgett *et al.*, Unusual transformations in the biosynthesis of the antibiotic phosphinothricin tripeptide. *Nat. Chem. Biol.* **3**, 480–485 (2007).
67. Y. Qi, E. Ding, J. A. V. Blodgett, Native and engineered clifednamide biosynthesis in multiple *Streptomyces* spp. *ACS Synth. Biol.* **7**, 357–362 (2018).
68. B. Ko *et al.*, Construction of a new integrating vector from actinophage ϕOZJ and its use in multiplex *Streptomyces* transformation. *J. Ind. Microbiol. Biotechnol.* **47**, 73–81 (2020).
69. J. A. V. Blodgett *et al.*, Common biosynthetic origins for polycyclic tetramate macrolactams from phylogenetically diverse bacteria. *Proc. Natl. Acad. Sci. U.S.A.* **107**, 11692–11697 (2010).
70. A. Delazar *et al.*, Iridoid glycosides from *Eremostachys glabra*. *J. Nat. Prod.* **67**, 1584–1587 (2004).
71. S. Cao *et al.*, Cytotoxic and other compounds from *Didymochlaena truncatula* from the Madagascar rain forest. *J. Nat. Prod.* **69**, 284–286 (2006).
72. T. Keiser, M. Bibb, M. Buttner, K. Chater, D. Hopwood, *Practical Streptomyces Genetics* (The John Innes Foundation, Norwich, 2000).
73. C. S. Li *et al.*, NF-κB inhibitors, unique γ-pyranol-γ-lactams with sulfide and sulfoxide moieties from Hawaiian plant *Lycopodiella cernua* derived fungus *Paraphaeosphaeria neglecta* FT462. *Sci. Rep.* **7**, 10424 (2017).